Promoting Effect of TiO₂ on the Hydrodenitrogenation Performance of Nickel Phosphide

Xiang Li,[†,‡] Mohong Lu,[†] Anjie Wang,*[,†,‡] Chunshan Song,[§] and Yongkang Hu[‡]

State Key Laboratory of Fine Chemicals, Dalian University of Technology, 158 Zhongshan Road, Dalian 116012, People's Republic of China, Liaoning Key Laboratory of Petrochemical Technology and Equipments, Dalian University of Technology, 158 Zhongshan Road, Dalian 116012, People's Republic of China, and Clean Fuels and Catalysis Program, EMS Energy Institute and Department of Energy and Mineral Engineering, The Pennsylvania State University, 209 Academic Projects Building, University Park, Pennsylvania 16802

TiO₂-containing bulk Ni₂P catalysts (Ti$_x$-Ni₂P) were prepared by coprecipitation and in situ H₂ temperature-programmed reduction (TPR), and characterized by XRD, CO chemisorption, TEM, XPS, TPR, and NH₃-TPD. Their hydrodenitrogenation performances were studied by using quinoline and decahydroquinoline (DHQ) as the model molecules. Both the hydrogenation and C−N bond cleavage activities of Ni₂P were improved by the introduction of TiO₂. The TiO₂ species were mainly located separately on the surface of the catalysts and had strong interactions with surface Ni and P species. The reducibility of the precursors as well as the surface electronic properties of Ni₂P catalysts were affected by the addition of TiO₂. Ti$_x$-Ni₂P showed higher CO uptake but less acid sites than Ni₂P. The promoting effect of TiO₂ was discussed by considering the electronic interactions between surface Ti and Ni₂P species and changes in the adsorption geometries of quinoline, DHQ, as well as the partially hydrogenated intermediates over Ti$_x$-Ni₂P.

1. Introduction

Catalytic hydrotreating is an important refining process to remove sulfur, nitrogen, and oxygen from liquid hydrocarbon fuels.[1−3] The conventional hydrodesulfurization (HDS) and hydrodenitrogenation (HDN) catalysts are alumina-supported Mo or W sulfides promoted by Ni or Co. Generally, HDN is more difficult than HDS over these supported metal sulfides.[4]

Transition metal phosphides have recently been reported to be a new class of high-performance HDS and HDN catalysts.[5−7] Among the phosphides studied, Ni₂P was found to be the most active phase in the iron group compounds. Ni₂P crystallizes in the Fe₂P structure type.[8] The electron microscopy (EM) analysis indicated that its morphology is like a rough, irregular particle.[9] The structure of the phosphides can be probed by XRD, EXAFS, and ³¹P MAS NMR.[6] The metallic character of nickel phosphides classifies their large ³¹P NMR shifts as Knight shifts, which enables them to be distinguished from those of diamagnetic phosphates.[10] For unsupported Ni₂P, two isotropic chemical shifts at 1487 and 4076 ppm were observed due to the presence of two types of P atoms in the structure.[10] None of the structures of phosphides is a layered one, as is the case for MoS₂.[11] Therefore, the activities of the phosphides are supposed to be proportional to their surface areas.[11] The unsupported Ni₂P shows relatively low surface areas. The reported values, as determined by N₂ adsorption, ranged from 1 to 17 m²/g.[9,11−13] XPS investigation showed the binding energy (BE) of the nonoxidic Ni 2p₃/₂ band in Ni₂P (853.3) was between that of Ni metal (852.2 eV) and NiO (855.8 eV), whereas the BE of nonoxidic P 2p (129.7 eV) was somewhat lower than that of elemental P (130.1 eV).[13] The temperature-programmed reduction (TPR) measurements revealed that the transformation of oxidic precursor to Ni₂P starts with the formation of Ni metal from NiO, followed by the reduction of phosphates at higher temperatures to volatile P compounds that react with the Ni to Ni₂P, with Ni₃P and Ni₁₂P₅ as possible intermediates.[10] Rodriguez et al.[14] studied the formation of bulk and SiO₂-supported MoP, Ni₂P, and NiMoP by time-resolved XRD. They found that the formation of the metal phosphides occurred at temperatures between 600 an 800 °C, which was independent of the type of oxidic precursor used or the presence of silica as a support. Because the common species in all the cases are phosphate-type groups (PO$_x$), they suggested that reduction of PO$_x$ by hydrogen is the final and determining step in the formation of the phosphides.

However, contrary to the bimetallic sulfide catalysts, no apparent synergy effect between Ni(Co) and Mo(W) in transition metal phosphides was observed. Rodriguez et al.[14] found that MoNiP/SiO₂ was much less active than either MoP/SiO₂ or Ni₂P/SiO₂ for the HDS of thiophene. Sun et al.[15] studied the HDS of DBT over silica-supported MoP, Ni₂P, and NiMoP catalysts, but no synergetic effect was observed between the phosphided Ni and Mo atoms. Zuzaniuk and Prins[16] as well as Stinner et al.[11] reported that both supported and unsupported ternary phosphides, such as CoMoP and NiMoP, were less active than MoP and Co₂P in the HDN of *o*-propylaniline. However, when H₂S is introduced, CoMoP and NiMoP were more active than Co₂P and Ni₂P and remained so even after H₂S was removed, indicating Mo may have a beneficial effect under these conditions.[11] More recently, Abu and Smith[12] reported that introduction of a small amount of Co to bulk Ni₂P and MoP led to a significant increase in the direct desulfurization selectivity during the conversion of 4,6-dimethyldibenzothiophene. According to them, the changes in selectivity corresponded to the changes in the surface Brønsted acidity and the metal sites.

* Address correspondence to this author at the School of Chemical Engineering, Dalian University of Technology, Dalian 116012, People's Republic of China. Tel: +86-411-88993693. Fax: +86-411-88993693. E-mail: ajwang@dlut.edu.cn.

† State Key Laboratory of Fine Chemicals, Dalian University of Technology.

‡ Liaoning Key Laboratory of Petrochemical Technology and Equipments, Dalian University of Technology.

§ The Pennsylvania State University.

Hydrodenitrogenation of Nickel Phosphide

J. Phys. Chem. C, Vol. 112, No. 42, 2008 **16585**

They also studied the HDN of carbazole over Ni$_x$MoP,[17] but found that Ni$_x$MoP had a lower TOF, whereas the selectivity to bicyclohexane was higher for Ni$_x$MoP than for MoP. They attributed the increased C−N bond cleavage activity to the increase in the acidity of the catalyst.

Generally, the HDS activity of CoMo or NiMo sulfides supported on TiO$_2$-Al$_2$O$_3$ mixed oxides is superior to that of conventional γ-Al$_2$O$_3$ supported CoMo or NiMo sulfides.[18] Under these circumstances, TiO$_2$ also acts as a promoter. Both the reducibility and the sulfidability of these catalysts are improved by the addition of TiO$_2$ to γ-Al$_2$O$_3$. In the present work, we studied the promoting effect of TiO$_2$ on bulk Ni$_2$P in the HDN of quinoline (Q) and decahydroquinoline (DHQ), the fully hydrogenated intermediate in Q HDN. Quinoline was chosen as the model molecule because it is one of the typical basic nitrogen-containing compounds in oil fractions. Moreover, due to its molecular structure, all reactions that take place in an industrial HDN process also occur in the HDN network of quinoline, that is, C−N bond cleavage, hydrogenation of aromatic heterocyclic rings, and hydrogenation of benzenic rings.[19]

2. Experimental Methods

2.1. Preparation of Catalyst Precursors. The precursors of TiO$_2$-containing bulk Ni$_2$P were prepared by the coprecipitation method. In a typical procedure, 3.90 g of Ni(NO$_3$)$_2$·6H$_2$O (A. R. grade) was dissolved in 15 mL of deionized water. The required quantity of TiCl$_4$, dissolved in ethanol (0.14 mol/L), was added to the aqueous solution to form a clear solution. Subsequently, 1.77 g of (NH$_4$)$_2$HPO$_4$ (A. R. grade) dissolved in 10 mL of deionized water was added dropwise under stirring. After the addition of (NH$_4$)$_2$HPO$_4$ solution, the mixture was stirred while the water was evaporated to obtain a solid product. The resulting solid was further dried at 120 °C for 12 h and calcined at 500 °C for 6 h to obtain the final oxidic precursor. Compared with the stoichiometric Ni/P ratio, surplus P was used because of the loss of phosphorus during the reduction stage.[20] The TiO$_2$-containing nickel phosphides are denoted as Ti$_x$-Ni$_2$P, where x represents the Ti/Ni atomic ratio.

For comparison, a bulk Ni$_2$P and a mechanical mixture of P$_2$O$_5$ and TiO$_2$ (denoted as P-Ti) were also prepared. The atomic ratio of P/M (M = Ni or Ti) in the precursors was 1.

2.2. HDN Activity Measurement. Prior to HDN reaction, instead of the conventional ex-situ H$_2$ TPR method,[6] an in situ H$_2$ TPR method was used to transform the precursor into the active phase.[21] The precursor was pelleted, crushed, and sieved to 20−30 mesh. A total of 0.20 g of precursor was used for each run. The precursor was reduced in a 200 mL/min H$_2$ flow by heating from room temperature to 400 at 2 deg/min, then to 500 at 1 deg/min, and holding at 500 °C for 2 h.

After the precursor had been converted into a nickel phosphide, the reactor was cooled to the HDN reaction temperature. The HDN activities of the catalysts were investigated by using a solution of 1% (weight) Q or 0.8% (weight) DHQ in decalin (A. R. grade) as the model feed. The HDN reaction conditions were as follows: temperature 300−360 °C, total pressure 4 MPa, WHSV 24 h^{-1}, and H$_2$ flow 150 mL/min (at atmospheric pressure). Sampling of liquid HDN products was started 6 h after the reaction condition had been achieved. For each run, three to five liquid samples were collected at an interval of 20 min. The compositions of both feed and HDN liquid products were analyzed by an Agilent-6890N gas chromatograph equipped with an FID detector, using a commercial HP-5 column.

Scheme 1 shows the reaction network of quinoline HDN.[19] The conversion of Q to 1,2,3,4-tetrahydroquinoline (THQ1) is

SCHEME 1: Reaction Network of Quinoline HDN
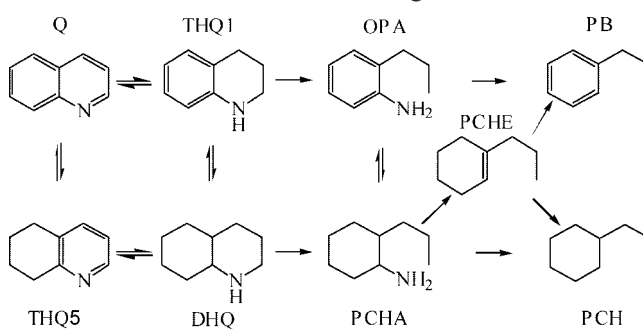
very fast, and most likely equilibrium is reached in every experiment.[22] Moreover, because there are several nitrogen-containing intermediates in the HDN of quinoline, such as THQ1, 5,6,7,8-tetrahydroquinoline (THQ5), *o*-propylaniline (OPA), and DHQ, conversions of Q or DHQ cannot be used to represent the HDN efficiency. Therefore, HDN conversion was used to measure the HDN efficiency of the catalysts:

$$\text{HDN conversion} = \frac{C_{N0} - C_{NR} - C_{NC}}{C_{N0}} \times 100$$

$$= \frac{\sum C_{HC}}{C_{N0}} \times 100 \tag{1}$$

where C_{N0} represents the concentration of reactant (Q or DHQ) in the feed, C_{NR} is the concentration of reactant (Q or DHQ) in the HDN liquid product, C_{NC} is the sum of the concentrations of all nitrogen-containing intermediates in the HDN liquid product, and $\sum C_{HC}$ is the sum of the hydrocarbon concentrations. The HDN conversion and CO uptake were used to calculate the HDN turnover frequency (HDN TOF) of the catalysts.

2.3. Catalyst Characterization. TPR profiles of the catalyst precursors were measured on a Chembet-3000 analyzer, using 0.10 g of calcined sample. Before the measurement, the sample was pretreated in He at 200 °C for 2 h. A gas mixture of 10% (volume) H$_2$ in Ar was used as the reacting agent and the TPR profiles of the catalysts were measured from 100 to 1000 at 10 deg/min.

The XRD patterns of the catalysts and P-Ti were measured on a Rigaku D/Max 2400 diffractometer with nickel-filtered Cu Kα radiation at 40 kV and 100 mA. Natural graphite was used as the internal standard to obtain absolute peak positions. Transmission electron microscopy (TEM) images of Ni$_2$P and Ti$_{0.03}$-Ni$_2$P were taken with a JEM-100CXII microscope at an accelerating voltage of 180 kV. X-ray photoelectron spectroscopy (XPS) spectra were obtained with a Multilab2000 X-ray photoelectron spectrometer, using an Mg Kα source. For the individual energy regions, a pass energy of 20 eV was used. All binding energies were referenced to the C 1s peak at 284.6 eV. Before the XRD, TEM, and XPS measurements, all the samples were prepared according to the same reduction conditions as used in the in situ reduction, followed by passivation with 0.5% (volume) O$_2$ in Ar.

The CO uptake was measured by using pulsed chemisorption according to the literature (12). About 0.2 g of passivated, air-exposed sample was rereduced in a H$_2$ flow to remove the passivation layer (80 mL/min flow rate, heating from 25 to 500 °C at a rate of 10 deg/min, and then being held at the final temperature for 1 h). The reactor was then cooled to 30 °C in a flow of H$_2$. An Ar flow at 80 mL/min was used to flush the catalyst for 30 min to achieve an adsorbate-free, reduced catalyst
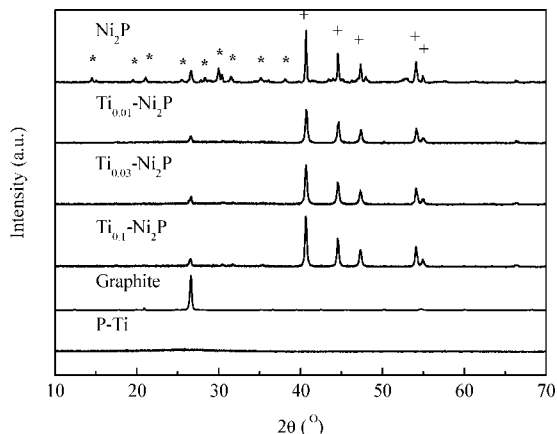
Figure 1. XRD patterns of the Ni_2P, Ti_x-Ni_2P, and P-Ti samples with natural graphite as the internal standard. (∗, $Ni_2P_4O_{12}$; +, Ni_2P).

TABLE 1: XRD Data of Ni_2P and Ti_x-Ni_2P

catalyst	*hkl*				
	(111)	(201)	(210)	(002)	(211)
Ni_2P	40.7	44.6	47.4	54.1	54.9
$Ti_{0.01}$-Ni_2P	40.7	44.6	47.4	54.2	55.0
$Ti_{0.03}$-Ni_2P	40.7	44.5	47.3	54.1	55.0
$Ti_{0.1}$-Ni_2P	40.6	44.5	47.3	54.0	54.9

surface. After pretreatment, 1.25 mL pulses of CO at a volume concentration of 1% in Ar were injected into a flow of Ar (80 mL/min), and the CO uptake was measured by using a TCD. CO pulses were repeatedly injected until the response from the detector showed no further CO uptake after consecutive injections.

NH_3 temperature-programmed desorption (NH_3-TPD) experiments were performed on a Chembet-3000 analyzer to determine the acid properties of the catalysts. Before TPD measurements, a 0.2 g passivated sample was rereduced in H_2 for 1 h at 500 °C, and was then cooled to 40 °C and exposed to NH_3 for 30 min. After the reactor was purged in a He flow, the temperature was raised at a linear rate of 10 deg/min to 500 °C.

3. Results

3.1. Characterization. The XRD patterns of the Ni_2P, Ti_x-Ni_2P samples, and natural graphite (the internal standard) are shown in Figure 1. A Ni_2P phase (powder diffraction file 74−1385) was present in the Ti_x-Ni_2P and Ni_2P catalysts. However, the bulk nickel phosphide sample also showed small amounts of impurities in the absence of TiO_2. These impurities are assigned to nickel phosphates, i.e., $Ni_2P_4O_{12}$ (powder diffraction file 76−1557). With the addition of TiO_2, only the typical diffraction patterns of Ni_2P were observed, indicating that the addition of a small amount of TiO_2 to the precursor favors the formation of Ni_2P. Its XRD pattern also demonstrates that the reduced P-Ti sample was present in an amorphous structure, suggesting that phosphorus does not react with titanium to form titanium phosphide under the conditions used to prepare nickel phosphides. Table 1 summarizes the XRD data of Ni_2P and Ti_x-Ni_2P. Neither lattice distortion nor peaks associated with nickel titanium phosphide (NiP_5Ti_2) were observed, indicating the TiO_2 and Ni_2P existed separately in Ti_x-Ni_2P, but not in the form of a solid solution.

Figure 2 shows the TPR profiles of the calcined oxidic precursors of P-Ti, Ni_2P, and Ti_x-Ni_2P. The temperatures of the TPR peaks of Ti_x-Ni_2P are summarized in Table 2. A small, broad peak at about 600 °C was observed for the P-Ti sample.
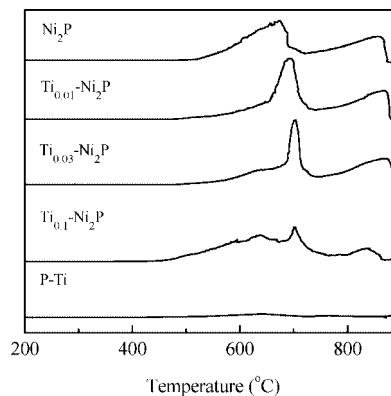

Figure 2. TPR profiles of Ni_2P, Ti_x-Ni_2P precursors, and P-Ti.

TABLE 2: Temperatures of the H_2 Consumption Peaks in the TPR Profiles of Ni_2P and Ti_x-Ni_2P

catalyst	main H_2 consumption peak temp (°C)
Ni_2P	675, 855
$Ti_{0.01}$-Ni_2P	722, 867
$Ti_{0.03}$-Ni_2P	629, 742, 872
$Ti_{0.1}$-Ni_2P	638, 701, 836

This can be attributed to the partial reduction of Ti^{4+} to low-valence Ti species.[23] The TPR profile of the Ni_2P precursor consisted of two main features, one at low temperature (675 °C) and the other at higher temperature (860 °C). The low-temperature peak corresponds to the reduction of nickel oxide to metallic nickel.[24] The high-temperature peak is assigned to the formation of nickel phosphides, the reduction of excess phosphate, or both.[25] In the presence of TiO_2, the low-temperature reduction peak became sharp and narrow and shifted to higher temperature, while the high-temperature reduction peak remained almost unaffected. Moreover, a broad shoulder appeared at 639 °C. The intensity of this shoulder peak increased with increasing Ti/Ni ratio.

NH_3-TPD was performed to investigate the acid properties of the Ni_2P and Ti_x-Ni_2P catalysts. The profiles are shown in Figure 3. The Ni_2P sample showed two peaks, one at a low temperature of 115 °C and the other at a high temperature of 315 °C. After the addition of TiO_2, the intensity of the high-temperature peak at 315 °C decreased remarkably.

The XPS spectra in the Ni(2p) and P(2p) regions for the reduced catalysts are shown in Figure 4. All spectra showed oxidized Ni and P species, because after synthesis the catalysts were passivated with 0.5% O_2 in Ar to protect them from deep oxidation. For Ni_2P, the bands at 857.9 (Figure 4a) and 134.8 eV (Figure 4b) are assigned to Ni^{2+} and P^{5+} species, respec-
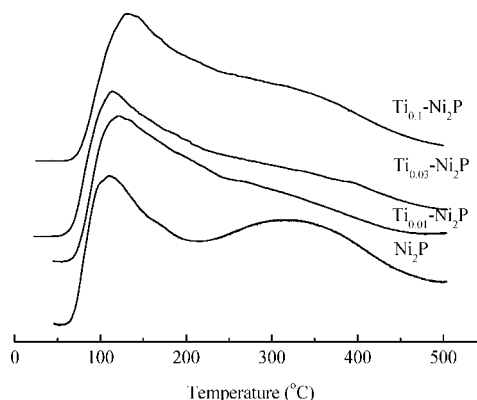

Figure 3. NH_3-TPD profiles of Ni_2P and Ti_x-Ni_2P.

Hydrodenitrogenation of Nickel Phosphide

J. Phys. Chem. C, Vol. 112, No. 42, 2008 **16587**
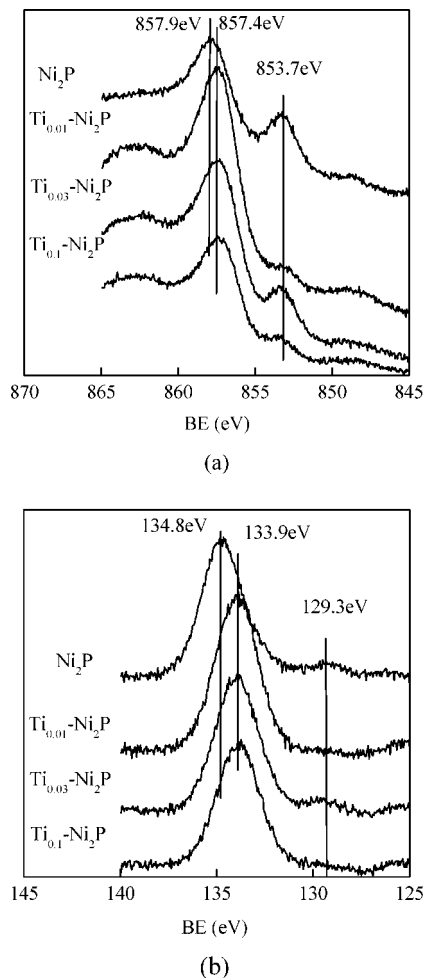

(a)

(b)

Figure 4. XPS spectra of (a) the Ni(2p) region and (b) the P(2p) region of Ni_2P and the Ti_x-Ni_2P catalysts after reduction and passivation.
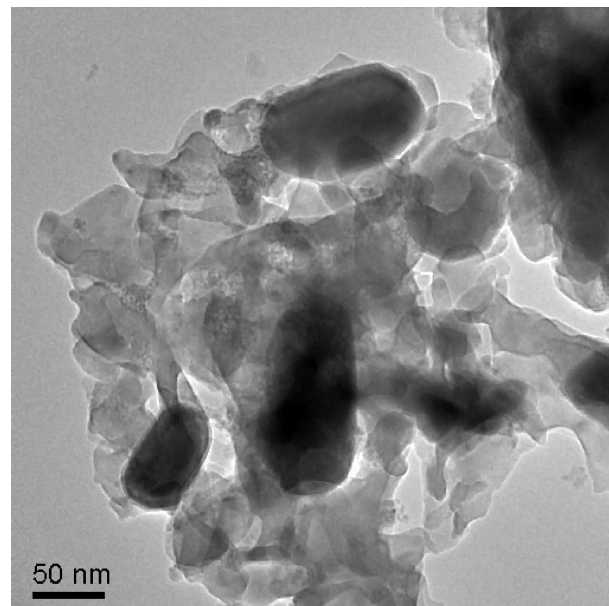
TABLE 3: CO uptake and Ti/Ni atomic ratio of Ti_x-Ni_2P and Ni_2P

	Ti/Ni atomic ratio			
catalyst	$r_n{}^a$	$r_{XPS}{}^b$	r_{XPS}/r_n	CO uptake ($\mu mol \cdot g^{-1}$)
Ni_2P	0	0		5.0
$Ti_{0.01}$-Ni_2P	0.01	0.04	4	5.1
$Ti_{0.03}$-Ni_2P	0.03	0.11	3.7	8.1
$Ti_{0.1}$-Ni_2P	0.10	0.20	2	7.0

^{a} r_n: the nominal Ti/Ni atomic ratio. ^{b} r_{XPS}: the Ti/Ni atomic ratio determined by XPS.

(a)

(b)

Figure 5. TEM images of Ni_2P (a) and $Ti_{0.03}$-Ni_2P (b).

tively, in the passivated layer formed on the surface of Ni_2P particles.[12,26] The peaks observed at 853.7 (Figure 4a) and 129.3 eV (Figure 4b) are assigned to reduced Ni and P species in Ni_2P.[12,26] In the presence of TiO_2, the BE of the surface Ni^{2+} species shifted from 857.9 to 857.4 eV (Figure 4a), and the BE assigned to the surface P^{5+} species shifted from 134.8 to 133.9 eV (Figure 4b). However, the binding energies assigned to reduced Ni and P species in Ni_2P were almost unaffected by the addition of TiO_2.

The relative surface Ti/Ni atomic ratios of the Ni_2P and Ti_x-Ni_2P samples determined by XPS (r_{XPS}) are presented in Table 3. The surface Ti/Ni atomic ratios of the Ti_x-Ni_2P samples were much higher than the corresponding nominal values (r_n), suggesting that Ti surface enrichment occurred upon reduction. On the other hand, as shown in Table 3, the r_{XPS}/r_n decreased with increasing TiO_2 content. For $Ti_{0.01}$-Ni_2P, the r_{XPS}/r_n was 4, while for $Ti_{0.1}$-Ni_2P the value decreased to 2.

Phosphide sites can be titrated by CO chemisorption at room temperature.[6] Irreversible CO uptake measurements were used to titrate the surface metal atoms and to provide an estimate of the active sites on the catalysts.[20] The measured CO adsorption capacities are presented in Table 3. The data show that the CO uptake of $Ti_{0.01}$-Ni_2P (5.1 $\mu mol/g$) was almost the same as that of Ni_2P (5.0 $\mu mol/g$). The maximum CO uptake (8.1 $\mu mol/g$) was observed for $Ti_{0.03}$-Ni_2P and then the value decreased with further increasing the content of TiO_2.

TEM images of Ni_2P and $Ti_{0.03}$-Ni_2P are shown in Figure 5. The Ni_2P particle size ranged from approximately 79 to 136 nm (Figure 5a), whereas the $Ti_{0.03}$-Ni_2P particles varied in size from 54 to 88 nm (Figure 5b). The Ni_2P particle size was decreased to some extent by the addition of TiO_2.

3.2. HDN of Quinoline. Figure 6 shows the variations of Q conversion with temperature during HDN catalyzed by Ni_2P and Ti_x-Ni_2P catalysts. At 300 °C, the conversion of Q was as
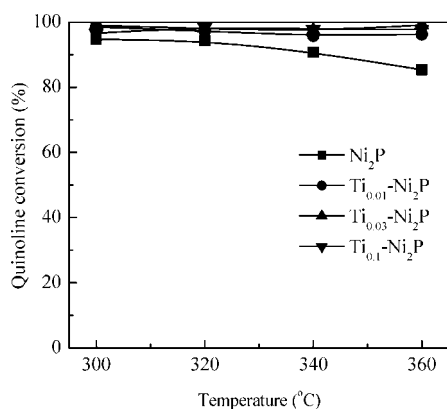
Figure 6. Quinoline conversion as a function of temperature over Ni_2P and Ti_x-Ni_2P.

high as 95% over Ni_2P, and then decreased with temperature. The addition of TiO_2 to Ni_2P led to a slight increase in the Q conversion. Even at 360 °C, the highest reaction temperature studied in the present work, the Q conversion over Ti_x-Ni_2P was only 12% larger than that over Ni_2P. Contrary to Ni_2P, the high Q conversion (>96%) over Ti_x-Ni_2P was almost constant in the whole temperature range studied.

Figure 7 illustrates the variation of the reactant and liquid product distributions in the HDN of Q with reaction temperature over the Ni_2P and Ti_x-Ni_2P catalysts. Although Q is very reactive, the liquid product distributions over these catalysts were quite different. THQ1 was the major product in the HDN of quinoline over Ni_2P (Figure 7a). Only small amounts of the other hydrogenated intermediates, THQ5 and DHQ (<5%), were detected. For Ti_x-Ni_2P, THQ1 was still the main hydrogenated intermediate, but its concentration decreased drastically. On the other hand, DHQ became the second most abundant hydrogenated intermediate and its concentration increased remarkably with increasing TiO_2 content. Especially for $Ti_{0.1}$-Ni_2P (Figure 7d), DHQ became the main product at low temperature (300 °C). In the HDN of Q over Ni_2P and Ti_x-Ni_2P, the concentrations of THQ1 and DHQ decreased with increasing temperature, except that a maximum of the concentration of THQ1 was observed at 320 °C for $Ti_{0.1}$-Ni_2P (Figure 7d). Moreover, it should be noted that the concentration of THQ5 also increased with increasing Ti/Ni atomic ratio.

Besides the fully hydrogenated intermediate (DHQ), concentrations of the C−N bond cleavage products, propylcyclohexane (PCH) and propylbenzene (PB), also increased with the increase in TiO_2 content. Above 340 °C, PCH and PB became the dominant compounds, and represented 66% of the reaction products over $Ti_{0.03}$-Ni_2P (Figure 7c). Further increase in the Ti/Ni ratio led to a decrease in the C−N bond cleavage products.

The variations of HDN TOF in the HDN of Q over Ni_2P and Ti_x-Ni_2P with temperature are shown in Figure 8. The HDN TOF of each catalyst increased with temperature, suggesting that the C−N bond cleavage is a thermodynamically favorable reaction. The HDN TOF also increased in the order Ni_2P < $Ti_{0.1}$-Ni_2P < $Ti_{0.03}$-Ni_2P < $Ti_{0.01}$-Ni_2P, indicating that the denitrogenation activity of Ni_2P was enhanced by the introduction of a small amount of TiO_2.

3.3. HDN of DHQ. Figure 9 shows the variation of the reactant and liquid product distributions in the HDN of DHQ with reaction temperature over the Ni_2P and Ti_x-Ni_2P catalysts. Ni_2P exhibited a low denitrogenation activity, no PB but only a small amount of PCH (<3%) was detected. The main products were the dehydrogenated N-containing molecules, i.e., THQ1,

THQ5, and Q. At temperatures below 320 °C, THQ1 was the most abundant compound. With increasing temperature, the concentration of THQ5 increased drastically, and THQ5 became the dominant product above 320 °C.

Ti_x-Ni_2P exhibited much higher C−N bond cleavage activity than Ni_2P. The concentrations of PB and PCH, the C−N bond cleavage products, increased with increasing Ti/Ni atomic ratio, and the formation of PCH was more enhanced by increasing the Ti content than that of PB. PCH became the most abundant product at Ti/Ni atomic ratios higher than 0.03. For $Ti_{0.03}$-Ni_2P, the yield of PCH reached 23% at 300 °C. THQ5 was the main dehydrogenated product over Ti_x-Ni_2P. No quinoline but only small amounts of THQ1 and OPA (both less than 3%) were detected. Among the Ti_x-Ni_2P catalysts, $Ti_{0.01}$-Ni_2P exhibited different catalytic behavior in DHQ dehydrogenation. The yield of THQ5 over $Ti_{0.01}$-Ni_2P was higher than that over $Ti_{0.03}$-Ni_2P and $Ti_{0.1}$-Ni_2P (Figure 9). Moreover, contrary to $Ti_{0.03}$-Ni_2P and $Ti_{0.1}$-Ni_2P, the concentration of THQ5 increased with temperature over $Ti_{0.01}$-Ni_2P. The results indicate that $Ti_{0.01}$-Ni_2P possessed higher dehydrogenation activity than $Ti_{0.03}$-Ni_2P and $Ti_{0.1}$-Ni_2P.

The variations of HDN TOF of Ni_2P and Ti_x-Ni_2P in the HDN of DHQ with temperature are shown in Figure 10. The HDN TOF of each catalyst increased with temperature, which confirmed that the C−N bond cleavage is a thermodynamically favorable reaction. The HDN TOF increased in the order Ni_2P < $Ti_{0.01}$-Ni_2P < $Ti_{0.03}$-Ni_2P < $Ti_{0.1}$-Ni_2P. Ni_2P showed a much lower HDN TOF than Ti_x-Ni_2P. The value was almost one order of magnitude lower than those of Ti_x-Ni_2P.

4. Discussion

4.1. Characterization. Among the methods used for preparing transition metal phosphide hydrotreating catalysts, such as the solid-state reaction of metal elements and phosphorus, the electrolysis of fused salts and the phosphidation of metals or metal oxides with PH_3/H_2,[27] the temperature-programmed reduction of metal phosphates by H_2 is the most commonly used one. This simple method, which was described in the 19th century for the preparation of unsupported metal phosphides, was first used by Robinson et al.[9] to prepare a phosphorus-promoted Ni/SiO_2 catalyst and was developed further by Oyama et al.[28] for metal phosphide hydrotreating catalysts. Generally, two steps are involved in the formation of transition metal phosphides with this method. One is the reduction of the transition metal oxide at the lower temperature region, whereas the other is the reduction of PO_x to elemental phosphorus and the formation of phosphide at higher temperature. According to Rodriguez et al.,[14] the reduction of PO_x is the final and determining step in the formation of transition metal phosphides. This reaction is thermodynamically unfavorable and kinetically slow because the P−O bond is strong, and its reduction requires very low heating rate and high temperature. As can be seen in the XRD patterns of Ni_2P (Figure 1), there still remained a small amount of phosphate ($Ni_2P_4O_{12}$), indicating that the reduction of PO_x was not fully accomplished after being reduced at 500 °C for 2 h. Addition of TiO_2 seems to facilitate the formation of Ni_2P, because peaks assigned to phosphate disappeared in the XRD patterns of Ti_x-Ni_2P.

The TPR profiles of Ni_2P and Ti_x-Ni_2P precursors (Figure 2) showed that the low-temperature H_2 consumption peak was more influenced by the introduction of TiO_2 than the high-temperature peak. The increased reduction temperature of the low-temperature peak in the TPR profiles of Ti_x-Ni_2P implies that a strong interaction may exist between Ti and Ni species. According to
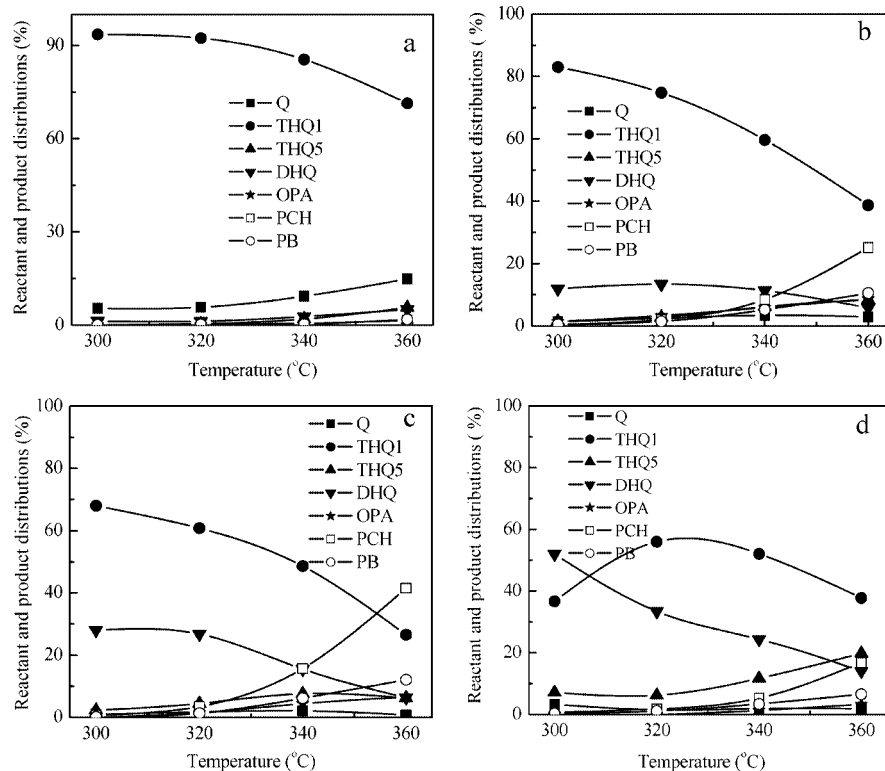
Hydrodenitrogenation of Nickel Phosphide

J. Phys. Chem. C, Vol. 112, No. 42, 2008 **16589**

Figure 7. Variations of reactant and liquid product distributions with temperature in quinoline HDN over Ni_2P (a), $Ti_{0.01}$-Ni_2P (b), $Ti_{0.03}$-Ni_2P (c), and $Ti_{0.1}$-Ni_2P (d).
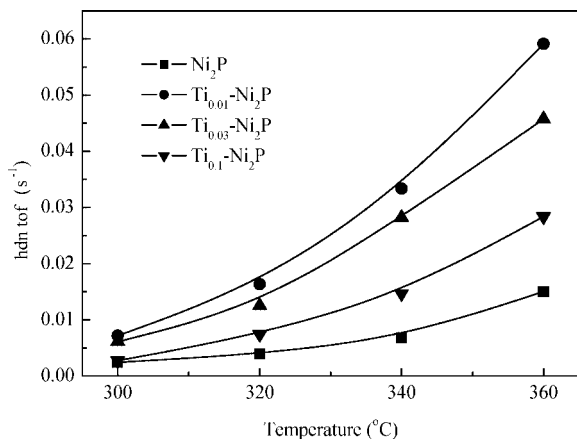

Figure 8. Variations of quinoline HDN TOF with temperature over Ni_2P and Ti_x-Ni_2P.

the relative surface Ti/Ni atomic ratios of the Ni_2P and Ti_x-Ni_2P samples determined by XPS (Table 3), these Ti species were mainly located on the surface of Ni_2P.

De Bokx et al.[29] studied the TPR of NiO supported on TiO_2. Two reduction peaks were observed for samples calcined above 300 °C. They attributed the low-temperature peak to the reduction of NiO and the high-temperature peak to the reduction of $NiTiO_3$, because $NiTiO_3$ is more difficult to reduce than NiO. According to them, NiO and TiO_2 interdiffused rapidly at calcination temperatures higher than 300 °C, and ultimately led to the formation of $NiTiO_3$. Damyanova et al.[30] also attributed the hydrogen consumption in the higher temperature region for NiO/TiO_2 to the reduction of octahedrally coordinated Ni^{2+} ions in a $NiTiO_3$-like structure. According to the TPR results and the distribution of Ti species determined by XPS, we assume that TiO_2 diffuses to the surface of the Ti_x-Ni_2P precursors to form a $NiTiO_3$ shell upon calcination at 500 °C in the oxidic

precursors, leading to the increase in the reduction temperature of the low-temperature peak. Once this surface $NiTiO_3$ shell is reduced, the reduction of bulk NiO in the Ti_x-Ni_2P precursors is accelerated, because at that moment the temperature is higher than required for the reduction of NiO, i.e. the system was in a "superheated" situation for the reduction of NiO. This could be the reason that the low-temperature peak in the TPR profiles of Ti_x-Ni_2P precursors became sharp and narrow. On the basis of the above discussion, the shoulder centered around 630 °C in the TPR profiles of $Ti_{0.03}$-Ni_2P and $Ti_{0.1}$-Ni_2P should be attributed to the reduction of NiO species. As shown in Table 3, the decreased r_{XPS}/r_n ratio indicates that surface segregation and growth of TiO_2 particles may take place with increasing Ti content, leaving part of the surface NiO species exposed to H_2 during reduction. Compared with the $NiTiO_3$ species, these NiO species are easier to reduce, and should be responsible for the appearance of the shoulder. On the other hand, the XRD (Figure 1 and Table 1) and XPS results suggested that following the formation of Ni_2P, the Ti-related species likely existed in the form of TiO_2 and reside on the surface of Ni_2P.

In the present study, the site densities of Ni_2P and Ti_x-Ni_2P were measured by using CO chemisorption and the obtained CO uptakes were used as the basis to calculate the HDN TOF of the catalysts in HDN. The results (Table 3) indicate that the number of surface active sites was significantly affected by the addition of TiO_2. The increase in CO uptakes of the catalysts with higher Ti/Ni ratio can also be attributed to the decreased particle size (Figure 5).

The negative shift of binding energies of surface Ni^{2+} and P^{5+} species (Figure 4) suggests the existence of an electronic effect caused by the surface Ti species, which may result in the electron enrichment on the surface Ni and P species. No significant shift in binding energy peaks assigned to the reduced Ni and P species in Ni_2P was observed (Figure 4), suggesting that the addition of TiO_2 did not affect the electronic properties
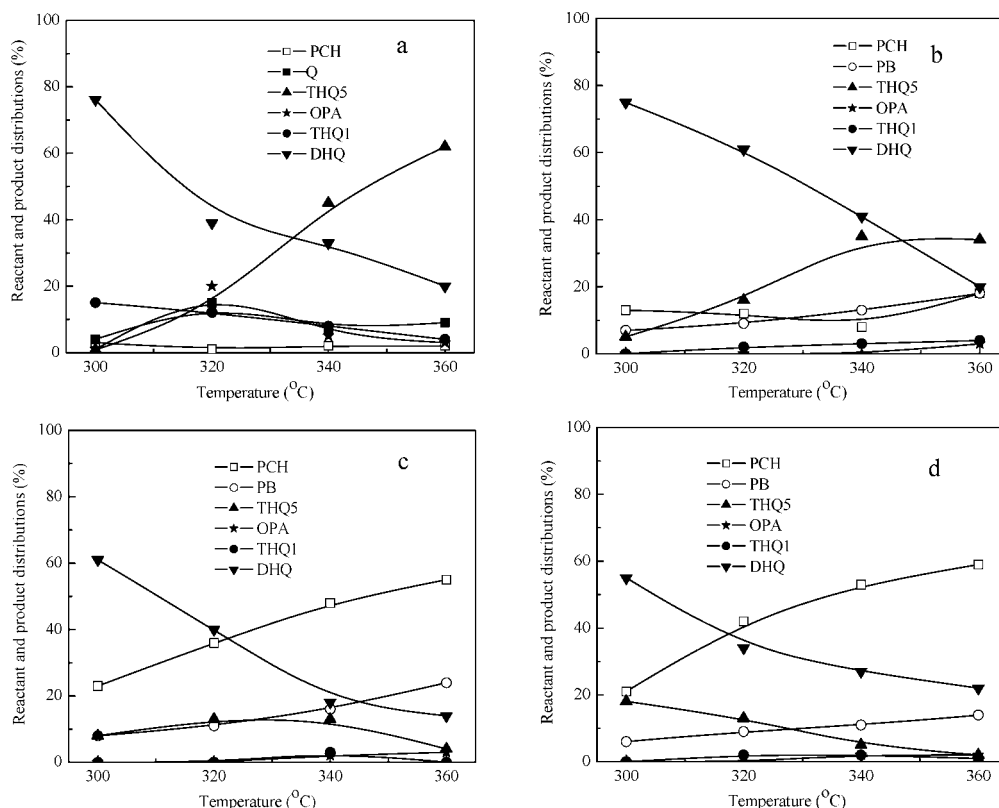
Figure 9. Variations of reactant and liquid product distributions with temperature in DHQ HDN over Ni_2P (a), $Ti_{0.01}$-Ni_2P (b), $Ti_{0.03}$-Ni_2P (c), and $Ti_{0.1}$-Ni_2P (d).

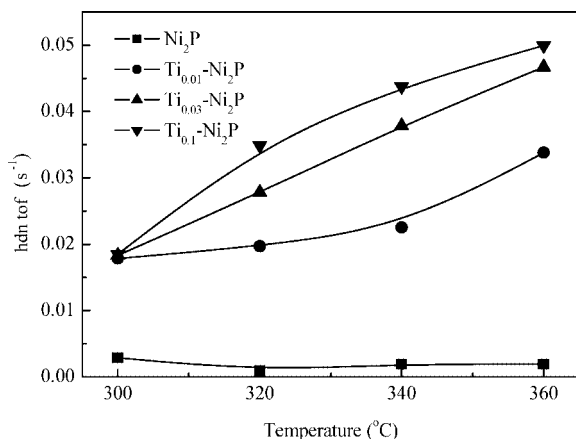**Figure 10.** Variations of DHQ HDN TOF with temperature over Ni_2P and Ti_x-Ni_2P.

of bulk Ni_2P, probably because the TiO_2 species were mainly located on the surface of the catalysts.

In conventional supported MoS_2 catalysts, TiO_2 is considered to be an electronic promoter.[31] Under HDS reaction conditions, a fraction of the Ti^{4+} species present in the support can be partially reduced to Ti^{3+} species. The 3d electron in Ti^{3+} can be easily transferred through the conduction band of the support and injected into the Mo 3d conduction band, leading to weakening of the Mo−S bond and an increase in the number of S vacancies or coordinatively unsaturated sites. In the TPR profile of P-Ti (Figure 2), a broad peak with low intensity related to the partial reduction of TiO_2 to low-valence Ti species was observed, suggesting that TiO_2 on the surface of Ti_x-Ni_2P can also be partially reduced. These low-valence Ti species on the surface of Ni_2P may act as the electron donor, and thus transform the surface Ni and P species to an electron-rich state.

Two distinct NH_3 desorption peaks at 109 and 315 °C were observed in the NH_3-TPD profile of Ni_2P (Figure 3). This is in agreement with the results of Wang,[32] who studied the temperature-programmed desorption of ethylamine over Ni_2P/SiO_2. The ethylamine-TPD profile was characterized by two desorption peaks with maxima at 107 and 361 °C, assigned to ethylamine desorption from physisorption sites and acid sites, respectively. Accordingly, the low-temperature peak and high-temperature peak in the NH_3-TPD profile of Ni_2P can be assigned to the desorptions of NH_3 from physisorption sites and acid sites of Ni_2P, respectively. The strength of the acid sites can be determined by the temperature at which the adsorbed NH_3 desorbs. On the basis of the desorption temperature, the acid sites are classified as weak (150−250 °C), medium (250−350 °C), or strong (350−450 °C).[33] Therefore, it can be concluded from the NH_3-TPD result that Ni_2P possesses moderate acidity. Lee and Oyama[34] also reported that Ni_2P/SiO_2 had moderate acidity in the form of PO-H sites. The high-temperature NH_3 desorption peak after addition of TiO_2 decreased markedly but was still located in the same temperature region. This observation suggested that the strength of acid sites of Ni_2P does not change by the addition of TiO_2 but the number of acid sites decreases drastically.

4.2. HDN. As shown in Scheme 1, the reaction network of quinoline HDN is complicated and consists of primary and secondary hydrogenation reactions, followed by C−N bond breaking reactions.[19] Figure 7 shows that the hydrogenation activity of bulk Ni_2P was enhanced by the addition of TiO_2, because DHQ was the second most abundant hydrogenated intermediate during quinoline HDN over Ti_x-Ni_2P, indicating that further hydrogenation of THQ1 took place. Over the Ni_2P catalyst THQ1 did not react further, but only reacted back to quinoline at higher temperature, because equilibrium at high temperature is on the side of the aromatic molecule. This is the

Hydrodenitrogenation of Nickel Phosphide

J. Phys. Chem. C, Vol. 112, No. 42, 2008 **16591**

reason for the decrease of the quinoline conversion over Ni_2P with temperature (Figure 6).

The enhanced hydrogenation activity of catalysts is often correlated with the enhanced acidity of the catalyst. Participation of Brønsted acidity in the hydrogenation is assumed in the heterolytic mechanism.[35,36] A reverse spillover mechanism where a proton is spilt over to a hydrogenation site may accelerate the hydrogenation.[37] In addition, strong adsorption of the aromatic ring on the acidic site next to the hydrogenation site may favor the hydrogenation.[38] However, this may not be true in our case, because the NH_3-TPD results indicated that the number of acid sites of Ni_2P catalysts decreased with the addition of TiO_2. The other possibility is that TiO_2 and the partially reduced low-valence Ti species on the surface of Ti_x-Ni_2P play a role as a Lewis base, weakening the adsorption of dihydro-intermediates (1,4-dihydroquinoline, 1,2-dihydroquinoline, or 3,4-dihydroquinoline) formed in the reaction of quinoline to THQ1 and thus facilitating the hydrogenation of quinoline. Campanati et al.[39] reported that the liquid phase hydrogenation of quinoline over Pd and Rh/Al_2O_3 catalysts under mild conditions was only partial and gave rise mainly to THQ1. The synthesis of the fully hydrogenated DHQ was not observed because of the irreversible adsorption of dihydro-intermediate(s) on the active sites. No modification was observed in this adsorption with increasing temperature and pressure or with the addition of a Brønsted acid or base. On the contrary, the addition of a strong and sterically hindered Lewis base allowed the partial formation of DHQ, hampering the irreversible adsorption of the dihydro-intermediate(s).

In catalytic HDN, it is generally accepted that nitrogen-containing molecules are adsorbed on the catalyst surface prior to reaction, and thus, the adsorptivities and adsorption configurations of the nitrogen-containing molecules affect their relative reactivities and the reaction pathways.[40,41] Quinoline can adsorb on the Ni-edge of NiMoS with the molecular plane parallel to the Ni-edge plane via side-on adsorption, or with the molecular plane perpendicular to the Ni-edge plane as end-on adsorption. A recent first principle study of heavy oil organonitrogen adsorption on NiMoS showed that quinoline is preferably adsorbed on the Ni-edge surface through the lone pair electrons of the nitrogen atom, which leads to a more ready hydrogenation of the nitrogen ring.[42] This is consistent with our observations that THQ1 was the major partially hydrogenated intermediate during quinoline HDN over Ni_2P and Ti_x-Ni_2P (Figure 7). Especially for Ni_2P, THQ1 was the most abundant compound and represented 71% of the reaction product at 360 °C. The concentration of THQ5, another partially hydrogenated intermediate, was only as low as 5.6% at 360 °C over Ni_2P, but it increased with increasing TiO_2 and reached 20% over $Ti_{0.1}$-Ni_2P at the same temperature, suggesting that the addition of TiO_2 facilitates the adsorption of quinoline with the side-on configuration.

The distribution of dehydrogenated products of DHQ HDN (Figure 9) indicates that the adsorption geometry of DHQ was also affected by the introduction of TiO_2 to Ni_2P. THQ1, THQ5, and quinoline were detected as the dehydrogenation products over Ni_2P. The concentration of THQ5 increased with temperature and became the main product above 320 °C, whereas THQ1 was the main dehydrogenation compound at low temperature (<320 °C). The formation of THQ1 was decreased by the addition of TiO_2. Only a small amount of THQ1 was detected in DHQ HDN over Ti_x-Ni_2P in the whole temperature range. The results suggest that adsorptions of DHQ with both the heterocyclic ring and the saturated carbon ring are possible

over Ni_2P. Especially at temperatures lower than 320 °C, it seems that DHQ tended to adsorb through the saturated carbon ring, leading to a relatively high yield of THQ1 after the dehydrogenation. On the contrary, at high temperature DHQ may prefer to interact with the surface of Ti_x-Ni_2P through the heterocyclic ring, yielding mainly THQ5. The addition of TiO_2 favors the adsorption of DHQ through the N-containing ring, which can be one of the reasons for the enhanced HDN TOF of Ti_x-Ni_2P in the HDN of DHQ (Figure 10).

Figure 8 shows that the HDN TOF of Ni_2P in Q HDN was also improved by the addition of TiO_2. Among the catalysts, $Ti_{0.01}$-Ni_2P exhibited the highest HDN TOF. The enhanced HDN TOF can be the result of both the enhanced C−N cleavage activity as well as the hydrogenation activity of Ti_x-Ni_2P. Because the C−N bond breaking occurs via DHQ, it is reasonable that the concentration of hydrocarbons increases as the reaction of THQ1 to DHQ speeds up. Therefore, the HDN of DHQ was carried out to evaluate the denitrogenation performance of Ni_2P and Ti_x-Ni_2P. For Ni_2P, only a small amount of PCH, one of the denitrogenation products, was detected (Figure 9). Ti_x-Ni_2P showed a much higher DHQ HDN TOF than Ni_2P, indicating that the C−N bond cleavage activity of Ni_2P was substantially improved by the addition of TiO_2. Moreover, the product distributions of DHQ HDN indicated that Ni_2P and $Ti_{0.01}$-Ni_2P possessed higher dehydrogenation activity, which should be responsible for the lower HDN TOFs for DHQ HDN than for Q HDN.

The Q and DHQ HDN results indicated TiO_2 is a promising promoter for Ni_2P in quinoline HDN. Both the C−N bond cleavage activity as well as the hydrogenation activity of Ni_2P can be enhanced by the introduction of TiO_2. Besides the adsorption configurations of the reactants, the acidity and the surface electronic properties are also important factors affecting the C−N bond cleavage activities of the hydrotreating catalysts. In the reaction network of quinoline HDN (Scheme 1), there are two irreversible reactions linked to THQ1 and DHQ. These two reactions are the first steps of the denitrogenation, in which a C−N bond is cleaved to form an aromatic (OPA) or aliphatic amine (propylcyclohexylamine, PCHA). PCHA is easily transformed into hydrocarbons and ammonia. A high-performance HDN catalyst should have high activity in breaking the hydrogenated heterocyclic ring.

There is a wealth of literature dealing with C−N bond cleavage reactions, which has been reviewed by Prins[40] and Oyama et al.[43] Mechanisms widely used to describe the cleavage of the C−N bond are nucleophilic substitution (S_N1, S_N2), elimination (E1, E2), and metallacycle or metal alkyl formation pathways. The pathways involving reactions with metals (C−N oxidative addition and metal alkyl formation) require activation of the α-carbon to the nitrogen.[44−46] These pathways likely occur with metallic catalysts such as Rh, Pd, or Ru but not with phosphide or sulfide catalysts.[20]

The molecules, the catalysts, and the reaction conditions all have been found to influence the mechanism.[47] Hadjiloizou et al.[48] proposed two mechanisms for piperidine ring opening: an E2 elimination and an S_N2 substitution. Both an acidic function of the catalyst (to bind the amine part of the reactant) and a basic function (to abstract the β-hydrogen atom) are needed in the elimination reaction.[40] Zhao et al.[49−51] found that over a sulfided $NiMo/\gamma$-Al_2O_3 catalyst, C−N bond cleavage of an alkylamine occurred exclusively by nucleophilic substitution by H_2S to form an alkanethiol. This substitution does not occur by a classic S_N2 substitution, but by a sequence of reactions in which the amine first dehydrogenates to an intermediate

imine.[52,53] Recently, Wang et al.[54] studied the HDN of 2-methylpyridine and its intermediates, 2-methylpiperidine as well as tetrahydromethylpyridine, over a sulfided NiMo/γ-Al$_2$O$_3$ catalyst. They considered the denitrogenation of 2-methylpiperidine to take place via substitution of 2-methylpiperidine to aminohexanethiols through imine intermediates. A recent study[43] on the HDN of 2-methylpiperidine over Ni$_2$P/SiO$_2$ and a commercial NiMoS/Al$_2$O$_3$ indicated that the mechanism of HDN on nickel phosphide is very similar to that on sulfides. The reaction proceeded in both cases predominantly by a substitution mechanism, with a smaller contribution of an elimination mechanism. However, for the more sterically hindered 2,6-dimethylpiperidine, the molecule reacted mainly by an E2 elimination process. Our NH$_3$-TPD results ruled out relations between the HDN activities and the surface acidities of Ti$_x$-Ni$_2$P, because the acidity of Ni$_2$P decreased with the addition of TiO$_2$. However, on the basis of XPS results, we cannot exclude the possibility that the increased electron density of surface Ni$_2$P species induced by the introduction of TiO$_2$ is responsible for the enhanced HDN activity of Ti$_x$-Ni$_2$P, because the electron-rich Ni$_2$P species are expected to enhance either the nucleophilic substitution or the abstraction of the β-hydrogen in the elimination reaction.

5. Conclusion

TiO$_2$ is a promising promoter for Ni$_2$P in Q and DHQ HDN, enhancing both the hydrogenation and C−N bond cleavage activities of Ni$_2$P. Among the Ti$_x$-Ni$_2$P catalysts, Ti$_{0.01}$-Ni$_2$P showed the highest Q HDN TOF but a low DHQ HDN TOF due to its high dehydrogenation activity. Characterization results indicated that the addition of TiO$_2$ facilitates the formation of Ni$_2$P. The TiO$_2$ species are mainly located separately on the surface of the catalyst and have strong interactions with surface Ni and P species. Both the reducibility of the precursors and the surface electronic properties of Ni$_2$P catalysts were affected by the addition of TiO$_2$. Ti$_x$-Ni$_2$P showed higher CO uptakes and a lower number of acid sites than Ni$_2$P. The product distributions suggested that the adsorption configurations of DHQ and Q were affected by the introduction of TiO$_2$. DHQ may prefer to interact with the surface of Ti$_x$-Ni$_2$P through the heterocyclic ring. The promoting effect of Ti, therefore, could be related to changes in the adsorption geometries of quinoline and DHQ, as well as the partially hydrogenated intermediates, and the electronic interactions between surface Ti and Ni$_2$P species.

References and Notes

(1) Knudsen, K. G.; Cooper, B. H.; Topsøe, H. *Appl. Catal. A* **1999**, *189*, 205.

(2) Song, C. S. *Catal. Today* **2003**, *86*, 211.

(3) Babich, I. V.; Moulijn, J. A. *Fuel* **2003**, *8*, 607.

(4) Kabe, T.; Ishihara, A.; Qian, W. *Hydrodesulfurization and Hydrodenitrogenation, Chemistry and Engineering*; Wiley-VCH: Weinheim, Germany, 1999.

(5) Phillips, D. C.; Sawhill, S. J.; Self, R.; Bussell, M. E. *J. Catal.* **2002**, *207*, 266.

(6) Oyama, S. T. *J. Catal.* **2003**, *216*, 343.

(7) Stinner, C.; Prins, R.; Weber, Th. *J. Catal.* **2000**, *191*, 438.

(8) Stinner, C. Novel, Binary and Ternary Transition-Metal Phosphides as Hydrodenitrogenation Catalysts, Ph.D. dissertation, Swiss Federal Institute of Technology Zurich, Zurich, 2001.

(9) Robinson, W. R. A. M.; Van Gestel, J. N. M.; Koranyi, T. I.; Eijsbouts, S.; Van der Kraan, A. M.; Van Veen, J. A. R.; De Beer, V. H. J. *J. Catal.* **1996**, *161*, 539.

(10) Stinner, C.; Tang, Z; Haouas, M.; Weber, Th.; Prins, R. *J. Catal.* **2002**, *208*, 456.

(11) Stinner, C.; Prins, R.; Weber, Th. *J. Catal.* **2001**, *202*, 187.

(12) Abu, I. I.; Smith, K. J. *J. Catal.* **2006**, *241*, 356.

(13) Korányi, T. I. *Appl. Catal. A* **2003**, *239*, 253.

(14) Rodriguez, J. A.; Kim, J. Y.; Hanson, J. C.; Sawhill, S. J.; Bussell, M. E. *J. Phys. Chem. B* **2003**, *107*, 6276.

(15) Sun, F.; Wu, W.; Wu, Z.; Guo, J.; Wei, Z.; Yang, Y.; Jiang, Z.; Tian, F.; Li, C. *J. Catal.* **2004**, *228*, 298.

(16) Zuzaniuk, V.; Prins, R. *J. Catal.* **2003**, *219*, 85.

(17) Abu, I. I.; Smith, K. J. *Catal. Today* **2007**, *125*, 248.

(18) Murali Dhar, G.; Srinivas, B. N.; Rana, M. S.; Kumar, M.; Maity, S. K. *Catal. Today* **2003**, *86*, 45.

(19) Jian, M.; Prins, R. *J. Catal.* **1998**, *179*, 18.

(20) Oyama, S. T.; Wang, X.; Lee, Y. K.; Bando, K.; Requejo, F. G. *J. Catal.* **2002**, *210*, 207.

(21) Wang, A.; Ruan, L.; Teng, Y.; Li, X.; Lu, M.; Ren, J.; Wang, Y.; Hu, Y. *J. Catal.* **2005**, *229*, 314.

(22) Satterfield, C. N.; Cocchetto, J. F. *Ind. Eng. Chem. Process Des. Dev.* **1981**, *20*, 53.

(23) Nagaoka, K.; Takanabe, K.; Aika, K. *Appl. Catal. A* **2003**, *225*, 13.

(24) Wang, X.; Clark, P.; Oyama, S. T. *J. Catal.* **2002**, *208*, 321.

(25) Lee, Y. K.; Shu, Y. Y.; Oyama, S. T. *Appl. Catal. A* **2007**, *322*, 191.

(26) Sawhill, S. J.; Phillips, D. C.; Bussell, M. E. *J. Catal.* **2003**, *215*, 208.

(27) Yang, S.; Liang, C.; Prins, R. *J. Catal.* **2006**, *237*, 118.

(28) Li, W.; Dhandapani, B.; Oyama, S. T. *Chem. Lett.* **1998**, *27*, 207.

(29) De Bokx, P. K.; Bonne, R. L. C.; Geus, J. W. *Appl. Catal.* **1987**, *30*, 33.

(30) Damyanova, S.; Spojakina, A.; Jirativa, K. *Appl. Catal. A* **1995**, *125*, 257.

(31) Ramírez, J.; Macías, G.; Cedeño, L.; Gutiérrez-Alejandre, A.; Cuevas, R.; Castillo, P. *Catal. Today* **2004**, *98*, 19.

(32) Wang, X. Novel, High Activity Hydroprocessing Catalysts: Iron Group Phosphides, Ph.D. dissertation, Virginia Polytechnic Institute and State University, Blacksburg, VI, 2002.

(33) Rynkowski, J. M.; Paryjczak, T.; Lenik, M. *Appl. Catal. A* **1993**, *106*, 73.

(34) Lee, Y. K.; Oyama, S. T. *J. Catal.* **2006**, *239*, 376.

(35) Ramírez, J.; Vrinat, M.; Breysse, M.; Lacroix, M. *Appl. Catal.* **1989**, *52*, 211.

(36) Okamoto, Y.; Maezawa, A.; Imanaka, T. *J. Catal.* **1989**, *120*, 29.

(37) Yumoto, M.; Idei, K.; Watanabe, K.; Usui, K.; Yamazaki, H. *Jpn.-Chin. Joint Seminar Petroleum Refining Technol., Tokyo* **1995**, 31.

(38) Lecrenay, E.; Sakanishi, K.; Nagamatsu, T.; Mochida, I.; Suzuka, T. *Appl. Catal. B* **1998**, *18*, 325.

(39) Campanati, M.; Vaccari, A.; Piccolo, O. *J. Mol. Catal. A: Chem.* **2002**, *179*, 287.

(40) Prins, R. *Adv. Catal.* **2001**, *46*, 399.

(41) Perot, G. *Catal. Today* **1991**, *10*, 447.

(42) Sun, M. Y.; Nelson, A. E.; Adjaye, J. *Catal. Today* **2005**, *109*, 49.

(43) Oyama, S. T.; Lee, Y. K. *J. Phys. Chem. B* **2005**, *109*, 2109.

(44) Laine, R. M. *Catal. Rev.-Sci. Eng.* **1983**, *25*, 459.

(45) Chisholm, M.H. *Polyhedron* **1997**, *16*, 3071.

(46) Weller, K. J.; Fox, P. A.; Gray, S. D.; Wigley, D. E. *Polyhedron* **1997**, *16*, 3139.

(47) Cattenot, M.; Portefaix, J. L.; Afonso, J.; Breysse, M.; Lacroix, M.; Pérot, G. *J. Catal* **1998**, *173*, 366.

(48) Hadjiloizou, G. C.; Butt, J. B.; Dranoff, J. S. *Ind. Eng. Chem. Res.* **1992**, *31*, 2503.

(49) Zhao, Y.; Kukula, P.; Prins, R. *J. Catal.* **2004**, *221*, 441.

(50) Zhao, Y.; Prins, R. *J. Catal.* **2004**, *222*, 532.

(51) Zhao, Y.; Prins, R. *J. Catal.* **2005**, *229*, 213.

(52) Prins, R.; Zhao, Y.; Sivasankar, N.; Kukula, P. *J. Catal.* **2005**, *234*, 509.

(53) Kukula, P.; Dutly, A.; Sivasankar, N.; Prins, R. *J. Catal.* **2005**, *236*, 14.

(54) Wang, H.; Liang, C.; Prins, R. *J. Catal.* **2007**, *251*, 295.